

Performance of the RPC-based ALICE muon trigger system at the LHC

To cite this article: ALICE Collaboration *et al* 2012 *JINST* **7** T12002

View the [article online](#) for updates and enhancements.

You may also like

- [Performance of a resistive plate chamber equipped with a new prototype of amplified front-end electronics](#)
Massimiliano Marchisone
- [Automatic breast density classification using neural network](#)
D. Arefan, A. Talebpour, N. Ahmadijhad et al.
- [R&D studies on eco-friendly gas mixtures for the ALICE Muon Identifier](#)
A. Bianchi

Performance of the RPC-based ALICE muon trigger system at the LHC

On behalf of the ALICE collaboration

F. Bossù,^{a,1} M. Gagliardi^{a,2} and M. Marchisone^{a,b}

^aUniversità degli Studi and Sezione INFN di Torino,
Via Giuria 1, 10125 Torino, Italy

^bUniversité B. Pascal and LPC Clermont-Ferrand, CNRS-IN2P3,
24 Avenue des Landais, 63171 Aubière Cedex, France

E-mail: Martino.Gagliardi@cern.ch

ABSTRACT: The forward muon spectrometer of ALICE (A Large Ion Collider Experiment) is equipped with a trigger system made of four planes of Resistive Plate Chambers (RPC), arranged in two stations with two planes each, for a total area of about 140 m². The system provides single and di-muon triggers with suitable transverse momentum selection, optimised for the physics of quarkonia and open heavy flavour. In the first two years of data-taking at the Large Hadron Collider (2010 and 2011) the 72 RPCs were operated in highly saturated avalanche mode in both pp and Pb-Pb collisions. The integrated charge was about 1.3 mC/cm² on average and 3.5 mC/cm² for the most exposed detectors. This paper describes two main results. The first result is the determination of the RPC performance, with particular focus on the stability of the main detector parameters such as efficiency, dark current, and dark rate. The second result is the measurement of the muon trigger performance in Pb-Pb collisions at $\sqrt{s_{NN}} = 2.76$ TeV, in terms of the reliability and stability of the trigger decision logic.

KEYWORDS: Trigger detectors; Muon spectrometers; Large detector systems for particle and astroparticle physics

We dedicate this piece of work to the memory of Anna Piccotti.

¹Now at iThemba LABS, Somerset West, South Africa.

²Corresponding author.

Contents

1	Introduction	1
2	Performance and stability of the ALICE muon trigger RPCs	2
2.1	Efficiency	2
2.2	Cluster size	3
2.3	Counting rate and current	3
3	Performance of the ALICE muon trigger system in Pb-Pb collisions	5
3.1	Multiplicities from the trigger algorithm	5
3.2	Muon trigger turn-on curve	7
3.3	Trigger selectivity	7
3.4	Muon tracking-trigger matching	8
4	Conclusions	10

1 Introduction

ALICE (A Large Ion Collider Experiment [1]) studies nuclear matter at very high temperatures and energy densities, and the transition to a deconfined partonic phase, known as Quark Gluon Plasma [2] (QGP). This is done via the analysis of ultra-relativistic heavy-ion collisions at the Large Hadron Collider (LHC). Proton-proton physics is also included in the ALICE program, both as a reference for observables measured in heavy-ion collisions and as a per se field of study.

Heavy flavour production is sensitive to the properties of QGP. In the ALICE forward muon spectrometer, heavy flavoured mesons are detected via their muonic and semi-muonic decays, in both Pb-Pb [3–5] and pp [6–9] collisions. The spectrometer is composed by a set of absorbers, a muon tracking system, a dipole magnet and a muon trigger system, whose task is to identify muons and to reduce the background of low transverse momentum (p_T) muons from light hadron decays. The muon trigger system consists of 72 Resistive Plate Chamber [10] (RPC) modules arranged in two stations, located, respectively, at a distance of 16 m and 17 m from the interaction point. Each station is made of two detection planes with 18 RPCs each. The detection planes are arranged perpendicular to the beam line. The total active area of the system is about 140 m². The total number of electronics channels is about 21000. The spatial information provided (with subcentimeter resolution [11]) by the RPCs is used to perform a selection on the muon p_T , via the deviation with respect to the trajectory of an infinite momentum track originated at the interaction point. The system is able to deliver single and di-muon (unlike- and like-sign) triggers. For each of these signals, two different p_T thresholds can be handled simultaneously, for a total of six trigger signals evaluated and delivered to the ALICE trigger processor at a frequency of 40 MHz and with a latency of about 800 ns. The first-level muon trigger decision is performed by a set of 234 electronics

boards. More details about the trigger algorithm and electronics are given in [12]. The fraction of operational Front-End Electronics (FEE) channels was 99.7% at the end of the 2011 data-taking.

In 2010 and 2011, ALICE took pp collision data at $\sqrt{s} = 7$ TeV (8 months/year)¹ and in Pb-Pb collisions at $\sqrt{s_{NN}} = 2.76$ TeV (1 month/year). In 2010, the typical luminosity in pp collisions was about $10^{29} \text{ cm}^{-2}\text{s}^{-1}$, corresponding to a single muon trigger rate of about 100 Hz, with a p_T threshold of 0.5 GeV/c. The luminosity in Pb-Pb collisions was about $10^{25} \text{ cm}^{-2}\text{s}^{-1}$. Given the low luminosity, no dedicated muon trigger was used in Pb-Pb collisions; however, the muon trigger data were read out and used for offline analysis. In 2011, the luminosity in pp collisions was about $2 \times 10^{30} \text{ cm}^{-2}\text{s}^{-1}$, corresponding to a single muon trigger rate of about 500 Hz and to a di-muon trigger rate of about 20 Hz, with a p_T threshold of 1 GeV/c. The luminosity in Pb-Pb collisions was about $3 \times 10^{26} \text{ cm}^{-2}\text{s}^{-1}$, corresponding to a single muon trigger rate of about 500 Hz and to a di-muon trigger rate of about 200 Hz, with a p_T threshold of 1 GeV/c.

2 Performance and stability of the ALICE muon trigger RPCs

The ALICE muon trigger detectors are 2 mm single gap RPCs, with low resistivity ($\simeq 10^9 \text{ }\Omega\text{cm}$) bakelite electrodes. They are operated in highly saturated avalanche mode [13], with a gas mixture consisting of 89.7% $\text{C}_2\text{H}_2\text{F}_4$, 10% C_4H_{10} , 0.3% SF_6 . The gas relative humidity is kept at 37%, in order to prevent alterations in the bakelite resistivity [14, 15]. The individual RPC areas range from $(72 \times 223) \text{ cm}^2$ to $(76 \times 292) \text{ cm}^2$. The signal is picked up inductively on both sides of the detector by means of orthogonal copper strips, in the X (bending plane) and Y (non-bending plane) directions. Strips with pitch of 1 cm, 2 cm and 4 cm and length ranging from 17 cm to 72 cm are employed; areas closer to the beam line have the finest segmentation. The RPC signal is discriminated in the FEE without pre-amplification [16]. The signal amplitude threshold of the FEE can be separately adjusted for each RPC via the Detector Control System (DCS); it is set to 7 mV for most RPCs.

The operating high voltage was optimised for each RPC with cosmic data, and fine-tuned with early pp collision data [14, 17]: the chosen values range from 10 kV to 10.4 kV. Operating voltage correction to compensate for temperature and pressure variations is performed online by the DCS.

In 2010 and 2011 the detectors were exposed to about 13 Mhit/cm² on average and 35 Mhit/cm² for the most exposed RPCs, corresponding to an integrated charge of 1.3 mC/cm² on average and 3.5 mC/cm² for the most exposed RPCs (as will be shown in 2.3, the average charge per hit is about 100 pC). Most of the hits were integrated in 2011. RPC prototypes operated with the same gas mixture have been ageing-tested [13, 18] up to an exposure of 550 Mhit/cm², corresponding to about ten years of safe operation at the LHC in the expected running conditions.

2.1 Efficiency

The RPC efficiency can be measured from data: since the trigger algorithm requires tracks to have hits in three out of four detection planes, the efficiency of a detection element in a given plane can be obtained by using the remaining three planes as an external tracking system [19].

In order to check the stability of the efficiency plateau, two high voltage scans were performed within 8 months from one another. A very good reproducibility of the efficiency curve was

¹In 2011, data were also taken for a few days in pp collisions at $\sqrt{s} = 2.76$ TeV.

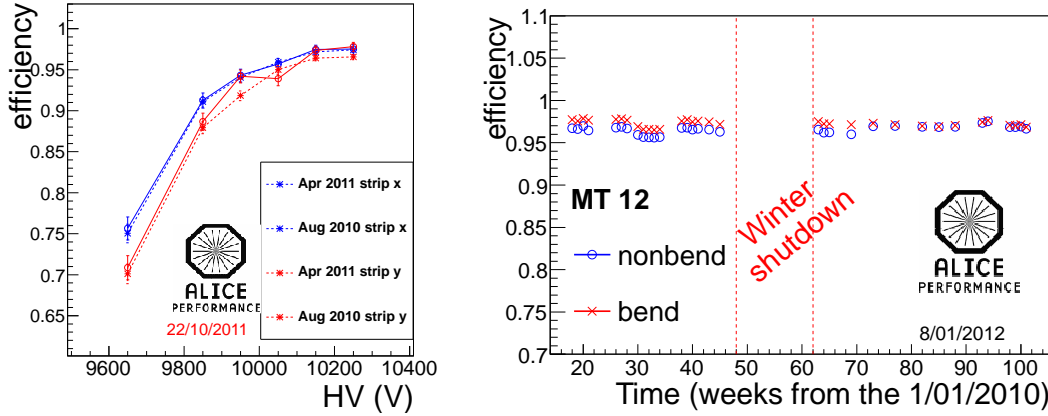


Figure 1. Left: efficiency curve of one RPC, as measured with pp collisions in two different high voltage scans 8 months apart. High voltage values are corrected by temperature and pressure variations. Right: average efficiency of one of the four detection planes (18 RPCs), as a function of time, in 2010 and 2011. The efficiency is measured separately for the X (bending) and Y (non-bending) planes.

observed (an example is shown in figure 1, left). The measured shift of the working point was less than 50 V ($\simeq 0.5\%$) for all RPCs.

The RPC efficiency is constantly monitored in order to provide efficiency maps for offline analysis and to check its stability in time. The results are summarised in figure 1, right: the average RPC efficiency, about 95%, has been stable within 0.5% in two years of operation.

2.2 Cluster size

The RPC cluster size was measured in both pp and Pb-Pb collisions. The results obtained with 2010 data are shown in figure 2 for the three different strip pitches employed in the RPCs.

The measured average value for strips of 2 cm is 1.40, in good agreement with the value of 1.33 measured in beam tests [13] during the R&D phase. The slight difference is compatible with the fact that the FEE threshold was set to 10 mV in the beam test and 7 mV in the current setup. No significant difference was found between the cluster size measured in pp and Pb-Pb collisions. The same analysis was performed with 2011 data, with compatible results.

2.3 Counting rate and current

The RPC dark current and counting rate were periodically monitored. The results are depicted in figure 3. The dark counting rate was measured from scalers, in dedicated runs taken right after the physics fills. Its average value of 0.05 Hz/cm² is very stable in time. The spikes seen in the autumn of 2011 can be ascribed to beam-induced afterglow, since in this period the LHC proton beams reached the highest intensity [20]; in the following Pb-Pb run (November 2011), with much lower intensities, the dark rate is again very stable. The average dark current shows a slightly increasing trend, which seems to be temporarily inverted or mitigated by long periods with high voltage turned off (e.g. the winter shutdown); the average value is 1.5 μ A, corresponding to about 0.1 nA/cm².

The maximum average current and counting rate reached during data-taking were measured to be about 1 nA/cm² and 10 Hz/cm², respectively. In such conditions (autumn 2011), the RPC

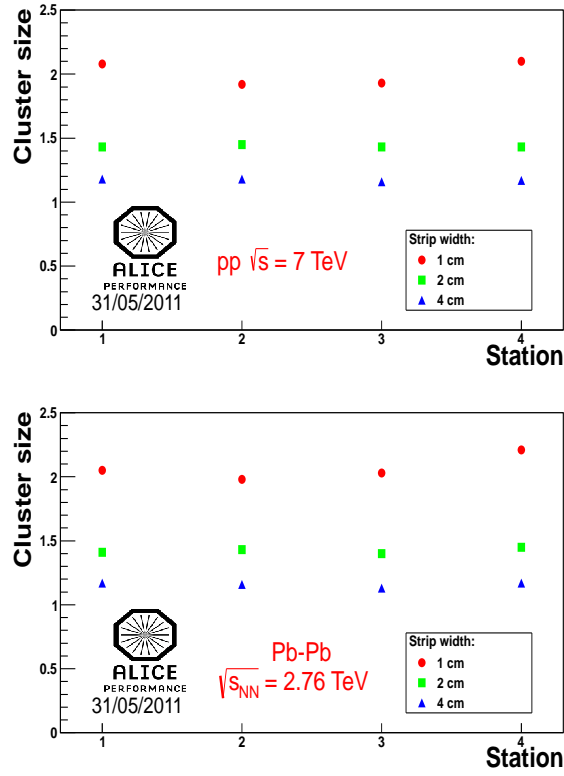


Figure 2. Average RPC cluster size for the four detection planes (18 RPC/plane), for strips with pitch 1 cm, 2 cm and 4 cm, in pp collisions at $\sqrt{s} = 7$ TeV (top) and in Pb-Pb collisions at $\sqrt{s_{NN}} = 2.76$ TeV (bottom).

currents and rates are dominated by the machine-induced background [21]. Beam tests [13, 18] have shown that the RPC performance are unaffected up to rates of about 80 Hz/cm².

In figure 4 the average RPC current during physics data-taking is plotted as a function of the average counting rate: as expected, a linear correlation is found. The slope of the curve is about 2 μ A/(Hz/cm²), corresponding to an average charge per hit of about 100 pC.

Figure 5 shows the RPC counting rate as a function of the minimum bias trigger rate in Pb-Pb collisions. The three curves correspond to the most exposed RPC, to the average of the RPCs on the most exposed detection plane and to the average of all RPCs. The slope of the curve corresponds to the average number of hits per minimum bias event: this quantity is 0.5×10^3 cm⁻² on average and 0.8×10^3 cm⁻² for the most exposed RPC. An extrapolation to 50 kHz minimum bias rate (hypothetical scenario for an upgraded LHC [22]) leads to counting rates of 25 Hz/cm² on average and 40 Hz/cm² for the most exposed RPC. Such rates are still tolerable by the detectors in terms of rate capability. However, the detector lifetime in such a scenario might be limited: thus, the possibility of switching to a lower-gain gas mixture and a new FEE with amplification in order to reduce ageing effects is being considered.

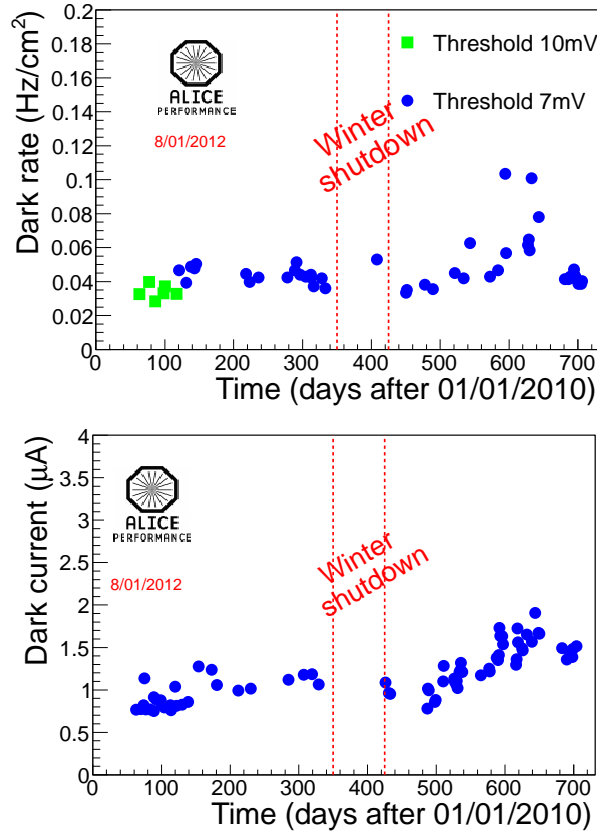


Figure 3. Average RPC dark rate (top) and dark current (bottom) as a function of time in 2010 and 2011.

3 Performance of the ALICE muon trigger system in Pb-Pb collisions

In this section the measured muon trigger multiplicities in Pb-Pb collisions and the performance of the trigger algorithm in 2010 and 2011 are described.

3.1 Multiplicities from the trigger algorithm

In figure 6 the muon multiplicity (average number of muons detected by the trigger algorithm per Pb-Pb collision) is shown for different centrality bins, ranging from 0-10% (most central) to 40%-80% (most peripheral). The centrality is measured as described in [23]. Muons are required to satisfy the trigger condition with the lowest possible p_T threshold ($p_T \simeq 0.5$ GeV/c) and to match a reconstructed track in the tracking system. The multiplicity is shown as a function of the LHC fill number, for a time span corresponding to about one month in both 2010 and 2011.

As expected, we observe that the muon multiplicity increases with the Pb-Pb collision centrality, since so does the number of binary nucleon-nucleon collisions. The stability of the detector response over time is satisfactory; the visible structures can be explained by slight changes in the number of active channels in the muon tracking system, affecting the muon reconstruction efficiency.

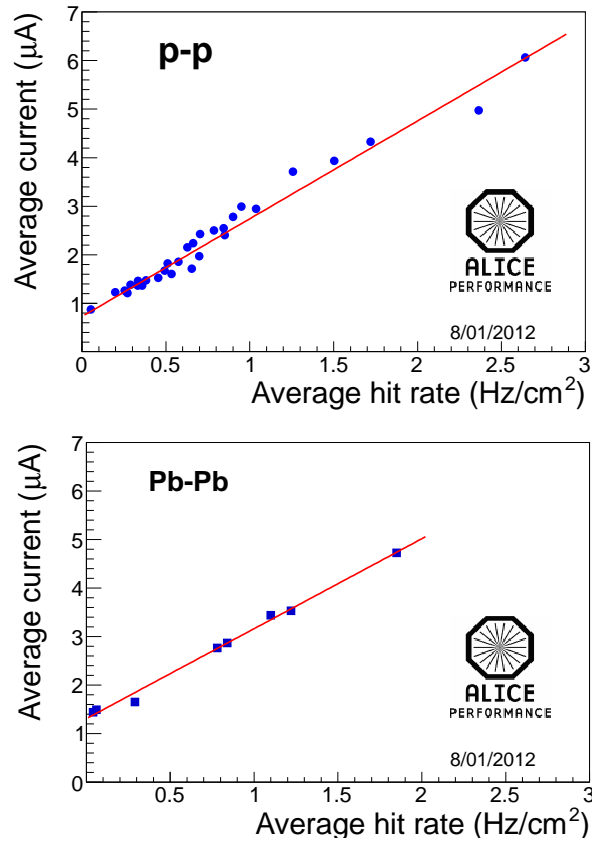


Figure 4. RPC average current as a function of the average counting rate in pp (top) and Pb-Pb (bottom) collisions, with superimposed linear fit. The fitted slopes are $2 \mu\text{A}/(\text{Hz}/\text{cm}^2)$ for pp collisions and $1.9 \mu\text{A}/(\text{Hz}/\text{cm}^2)$ for Pb-Pb collisions.

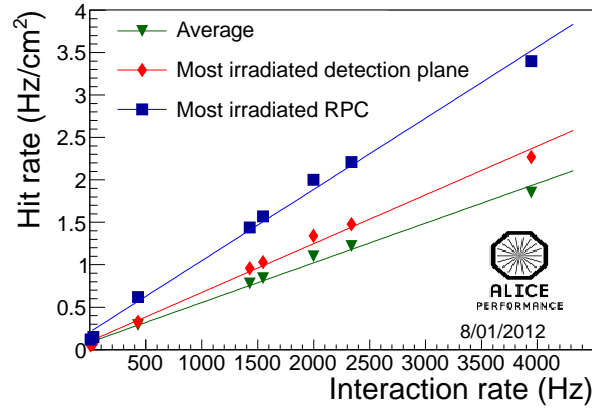


Figure 5. RPC counting rate as a function of the interaction rate in Pb-Pb collisions: for the most exposed RPC (blue squares); average for the RPCs on the most exposed detection plane (red dots); average for all RPCs (green triangles). Lines are linear fits to the data.

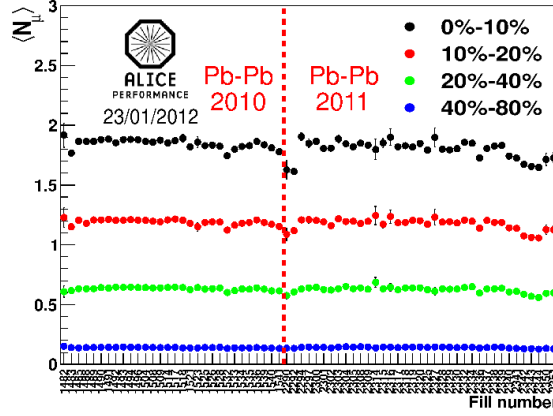


Figure 6. Average number of muons from the trigger algorithm as a function of the fill number, for various Pb-Pb collision centrality bins.

3.2 Muon trigger turn-on curve

The p_T thresholds are fixed by physics and bandwidth considerations. They are defined as the muon p_T for which an efficiency of 50% is reached. In 2010 (2011) the low- p_T threshold was set to 0.5 GeV/c (1 GeV/c) and the high- p_T threshold to 1 GeV/c (4 GeV/c). The hardware settings corresponding to the chosen thresholds are determined by simulation with muons of known transverse momentum [24]. In real data, the nominal high- p_T thresholds can be verified by measuring the trigger turn-on curves. The curves are obtained by the ratio of the reconstructed muon p_T distribution in the high- p_T muon sample to the reconstructed muon p_T distribution in the low- p_T sample. The reconstructed p_T is measured by the muon tracking system. The measured ratios for Pb-Pb collisions in 2010 and 2011 are shown in figure 7.

A plateau with saturation value close to unity is seen for large p_T values. As expected, the p_T values corresponding to a value of the ratio of 0.5 are close to the requested values of 1 GeV/c and 4 GeV/c. The behaviour of the ratios at very low p_T can be attributed to the fact that low- p_T muons passing through the muon filter² placed between the two subdetectors can be affected by multiple scattering effects causing them to be flagged as high- p_T tracks by the trigger algorithm.

3.3 Trigger selectivity

Figure 8 shows the trigger selectivity as a function of centrality, for different p_T thresholds. The trigger selectivity is defined as the ratio between the number of minimum bias events containing at least one muon with p_T larger than the threshold and the total number of events within a given centrality range.

As expected, the selectivity is lower in the most central classes, where, as shown in 3.1, muon production is enhanced by the large number of nucleon-nucleon collisions. In table 1 the trigger selectivities for two centrality bins are reported. The agreement between the 2010 and 2011 ratios with the same threshold is satisfactory; the small (1.5%) difference seen between the 2010 and

²The muon filter is a 1.2 m (7 hadronic interaction lengths) thick iron absorber located between the tracking and the trigger system.

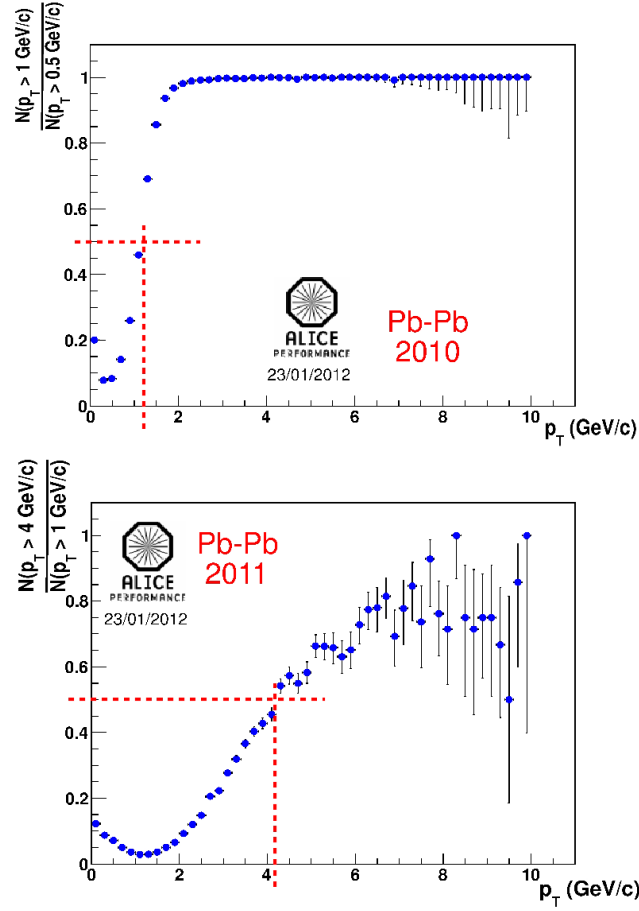


Figure 7. Muon trigger turn-on curves in Pb-Pb collisions for the 1 GeV/c threshold in 2010 (top) and for the 4 GeV/c threshold in 2011 (bottom).

Table 1. Trigger selectivity for two centrality ranges and different thresholds.

	2010 $p_T > 1 \text{ GeV/c}$	2011 $p_T > 1 \text{ GeV/c}$	2011 $p_T > 4 \text{ GeV/c}$
0%-10%	$(61.8 \pm 0.1)\%$	$(60.9 \pm 0.1)\%$	$(13.61 \pm 0.05)\%$
40%-80%	$(5.81 \pm 0.02)\%$	$(5.88 \pm 0.02)\%$	$(0.73 \pm 0.01)\%$

2011 selectivities in the most central collisions can be ascribed to slight variations in the fraction of unavailable channels or the RPC efficiency, affecting the overall trigger efficiency.

3.4 Muon tracking-trigger matching

Figure 9 shows the ratio of the number of tracks detected by both the muon tracking and the muon trigger system (matched tracks) to the number of tracks detected by the tracking system, as a function of p_T , for minimum bias events, in 2010 (top) and 2011 (bottom).

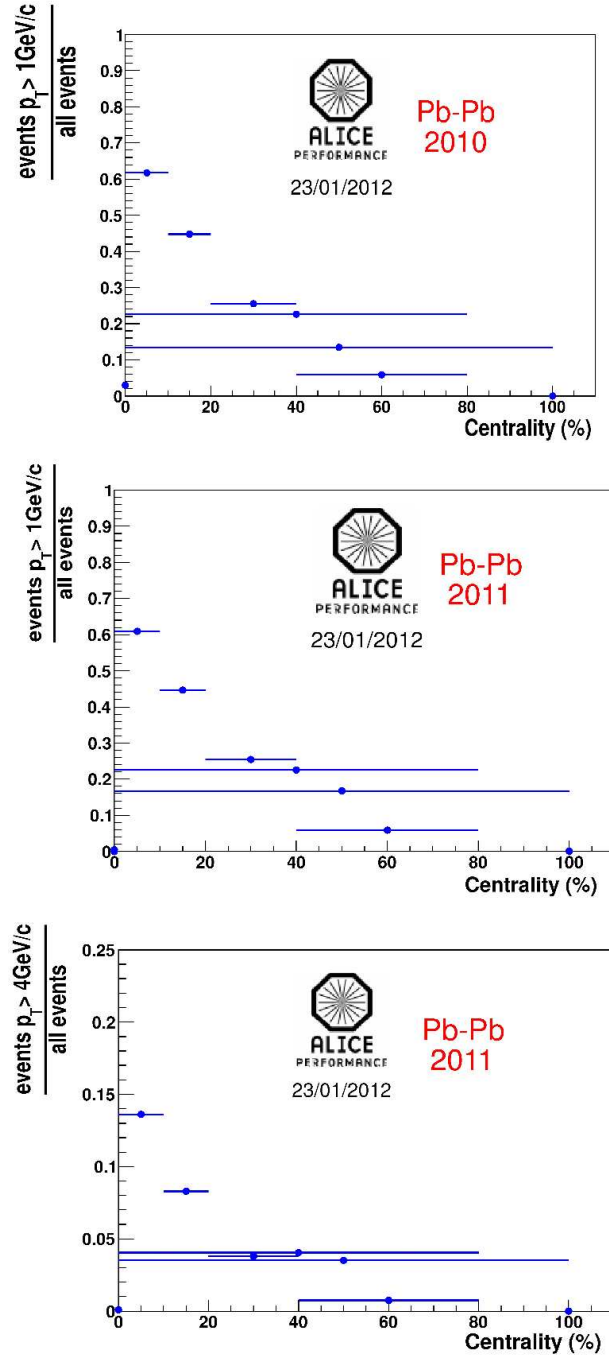


Figure 8. Muon trigger selectivities in Pb-Pb collisions in 2010 and 2011, with p_T thresholds of 1 GeV/c (top, center) and 4 GeV/c (bottom). The horizontal error bars represent the width of the centrality bin.

The results obtained for the two years are very similar. We note that the ratio does not reach unity, the saturation value at high p_T being $\simeq 0.85$. According to Pb-Pb collision simulations performed with the HIJING event generator, the fraction of unmatched tracks is largely accounted for by the contamination of hadrons in the sample of reconstructed tracks: these are stopped in the

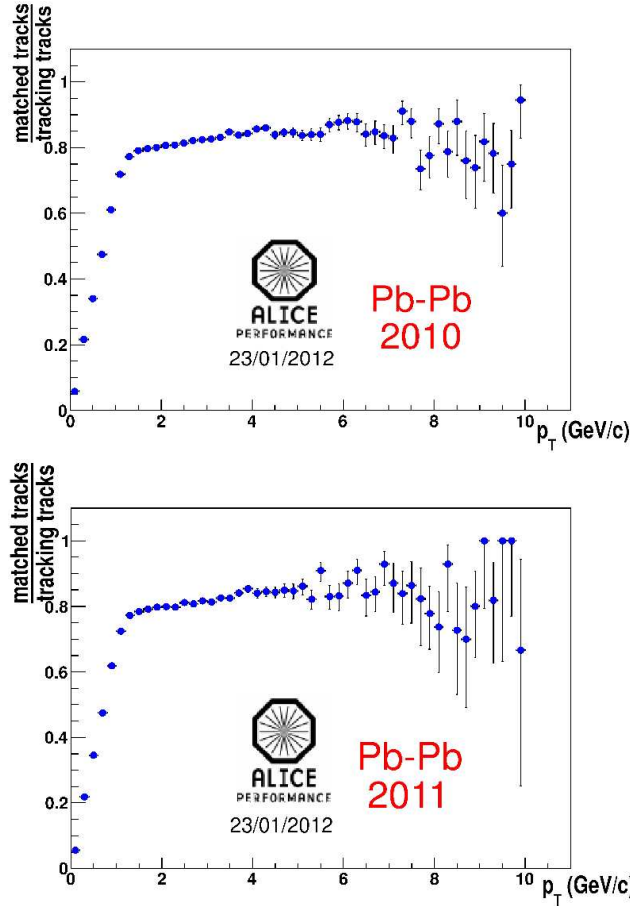


Figure 9. Number of matched tracks over the number of tracks detected at least by the muon tracking as a function of p_T for 2010 (top) and 2011 (bottom) Pb-Pb collisions.

muon filter and are not detected by the trigger system. Other effects, such as trigger and matching inefficiencies and tracks from beam-gas interactions, play a marginal role in defining the value of the ratio.

4 Conclusions

The ALICE muon trigger system has been fully operational during the first two years of data-taking at the LHC. The observed RPC performance are in agreement with the design values. The average RPC efficiency is about 95%; the cluster size is 1.4 with 2 cm wide strips; the dark current is about 0.1 nA/cm² and the dark counting rate is about 0.05 Hz/cm². The values of all these parameters are remarkably stable in time, with the sole exception of the dark current.

From the analysis of 2010 and 2011 muon trigger data in Pb-Pb collisions it is possible to conclude that: the muon trigger system has shown a stable behavior; the trigger decision algorithm is reliable and selective; the muon trigger is very efficient in rejecting hadrons detected by the muon spectrometer tracking system: it actually acts as a muon identifier.

The ALICE muon spectrometer is playing a crucial role in the ALICE physics program and, also in virtue of the performance and stability of the muon trigger system, is expected to continue to do so in the next years of LHC operation.

References

- [1] ALICE collaboration, K. Aamodt et al., *The ALICE experiment at the CERN LHC*, 2008 *JINST* **3** S08002.
- [2] F. Karsch, *Lattice simulations of the thermodynamics of strongly interacting elementary particles and the exploration of new phases of matter in relativistic heavy ion collisions*, *J. Phys. Conf. Ser.* **46** (2006) 122 [[hep-lat/0608003](#)].
- [3] ALICE collaboration, B. Abelev et al., *Production of muons from heavy flavor decays at forward rapidity in pp and Pb-Pb collisions at $\sqrt{s_{NN}} = 2.76$ TeV*, *Phys. Rev. Lett.* **109** (2012) 112301.
- [4] ALICE collaboration, B. Abelev et al., *J/ ψ suppression at forward rapidity in pb-pb collisions at $\sqrt{s_{NN}} = 2.76$ TeV*, *Phys. Rev. Lett.* **109** (2012) 072301 [[arXiv:1202.1383](#)].
- [5] ALICE collaboration, C. Suire, *Quarkonia production in ALICE*, in proceedings of 5th international conference on hard and electromagnetic probes of high-energy nuclear collisions, to appear on *Nucl. Phys. A*, Cagliari Italy May 27–June 1 2012.
- [6] ALICE collaboration, K. Aamodt et al., *Rapidity and transverse momentum dependence of inclusive J/ ψ production in pp collisions at $\sqrt{s} = 7$ TeV*, *Phys. Lett. B* **704** (2011) 442 [[arXiv:1105.0380](#)].
- [7] ALICE collaboration, B. Abelev et al., *Inclusive J/ ψ production in pp collisions at $\sqrt{s} = 2.76$ TeV*, *Phys. Lett. B* **718** (2012) 295 [[arXiv:1203.3641](#)].
- [8] ALICE collaboration, B. Abelev et al., *J/ ψ polarization in pp collisions at $\sqrt{s} = 7$ TeV*, *Phys. Rev. Lett.* **108** (2012) 082001 [[arXiv:1111.1630](#)].
- [9] ALICE collaboration, B. Abelev et al., *Heavy flavour decay muon production at forward rapidity in proton-proton collisions at $\sqrt{s} = 7$ TeV*, *Phys. Lett. B* **708** (2012) 265 [[arXiv:1201.3791](#)].
- [10] R. Santonico and R. Cardarelli, *Development of resistive plate counters*, *Nucl. Instrum. Meth. A* **187** (1981) 377.
- [11] ALICE collaboration, R. Arnaldi et al., *Spatial resolution of RPC in streamer mode*, *Nucl. Instrum. Meth. A* **490** (2002) 51.
- [12] R. Arnaldi et al., *Design and performance of the ALICE muon trigger system*, *Nucl. Phys. Proc. Suppl. B* **158** (2006) 21.
- [13] R. Arnaldi et al., *Beam and ageing tests with a highly saturated avalanche gas mixture for the ALICE pp data taking*, *Nucl. Phys. Proc. Suppl. B* **158** (2006) 149.
- [14] ALICE collaboration, M. Gagliardi et al., *Commissioning and first performance of the resistive plate chambers for the ALICE muon arm*, *Nucl. Instrum. Meth. A* **661** (2012) S45.
- [15] ALICE collaboration, R. Arnaldi et al., *Ageing tests on the low-resistivity RPC for the ALICE dimuon arm*, *Nucl. Instrum. Meth. A* **508** (2003) 106.
- [16] ALICE collaboration, R. Arnaldi et al., *Front-end electronics for the RPCs of the ALICE dimuon trigger*, *IEEE Trans. Nucl. Sci.* **52** (2005) 1176.
- [17] M. Gagliardi et al., *Final results of the tests on the resistive plate chambers for the ALICE muon arm*, *Nucl. Instrum. Meth. A* **602** (2009) 740.

- [18] F. Poggio, *Beam and ageing tests of Resistive Plate Chambers for the ALICE muon spectrometer*, Ph.D. thesis, [CERN-THESIS-2006-105](#), Università degli Studi di Torino, Torino Italy (2006).
- [19] D. Stocco, *Development of the ALICE muon spectrometer: preparation for data taking and heavy flavor measurement*, Ph.D. thesis, [CERN-THESIS-2008-144](#), Università degli Studi di Torino, Torino Italy (2008).
- [20] M. Ferro-Luzzi, *Review of 2011 LHC run from the experiments perspective*, in proceedings of *The LHC Performance Workshop* (Chamonix 2012), Chamonix France February 6–10 2012.
- [21] F. Bossù, *The ALICE muon spectrometer: trigger detector performance and readiness for the first physics measurements*, Ph.D. thesis, [CERN-THESIS-2012-073](#), Università degli Studi di Torino, Torino Italy (2012).
- [22] ALICE collaboration, J. Wessels et al., *Will ALICE be running during the HL-LHC era?*, in proceedings of *The LHC performance workshop* (Chamonix 2012), Chamonix France February 6–10 2012.
- [23] ALICE collaboration, K. Aamodt et al., *Centrality dependence of the charged-particle multiplicity density at mid-rapidity in Pb-Pb collisions at $\sqrt{s_{NN}} = 2.76$ TeV*, *Phys. Rev. Lett.* **106** (2011) 032301 [[arXiv:1012.1657](#)].
- [24] ALICE collaboration, A. Blanc and P. Dupieux, *The trigger system of the ALICE muon spectrometer at the LHC*, *Nucl. Instrum. Meth. A* **604** (2009) 301.